The Seventh Asian-Pacific Symposium on Structural Reliability and Its Applications (APSSRA2020)
October 4–7 2020, Tokyo, Japan
T. Takada, I. Yoshida & T. Itoi (editors)

A Full-Probabilistic Safety Assessment Method for Existing RC Bridges

T. Kouta[1] and C. Bucher[2]

[1]*Shimizu Corporation. Email: t.kouta@shimz.co.jp*
[2]*Vienna University of Technology. Email: christian.bucher@tuwien.ac.at*

Abstract: Throughout their service life, bridges are exposed to various kinds of stressors such as aging, environmental stressors, and increasing traffic loads. It may result in the degradation of the structural reliability of the bridges, leading ultimately to structural failure. Nowadays, an increasing number of bridges have been aging, and assessing them has become a big social concern. The safety of the structures depends on loads and resistances, both of which present several kinds of uncertainties. Therefore, in order to estimate structural safety, they should be considered as random variables. This study contributes to the development of a novel full-probabilistic safety assessment method for existing reinforced concrete (RC) bridges. In the proposed method, chloride-induced corrosion of reinforcement is considered as an important deterioration mechanism for RC bridges, and the resistances of the bridges are calculated as random variables. Meanwhile, weigh-in-motion (WIM) data are used to estimate stochastic traffic load models. As with most current design codes, axle concentrated loads and uniformly distributed loads are separately estimated. Then, the deterioration model and the traffic load model are applied to three-dimensional finite element (FE) analysis. Through the FE analysis, the structural reliability of the components of the bridges can be statistically and quantitatively evaluated. As a result of the study, the actual condition of the structures is quantitatively reflected to the reliability analysis.

Keywords: safety assessment, structural reliability, chloride-induced deterioration, weigh-in-motion data, finite element analysis.

1. Introduction

The highway transportation system has played an important role for modern society, and bridges are an essential component of it. The structural reliability of the bridges degrades over time due to various kinds of factors, such as aging, environmental stressors, and increasing traffic volumes. Recently, assessing such deteriorating bridges has become a big social concern because the number of those bridges has increased.

The reliability of structures depends on loads and resistances, both of which present several kinds of uncertainties. Therefore, in order to estimate structural safety, they should be treated as random variables.

Chloride-induced corrosion of reinforcing steels is one of the most significant deterioration mechanisms for reinforced concrete (RC) structures. In the past few decades, many experiments to explore chloride-induced corrosion mechanisms have been conducted, and several models have been developed and applied to some design codes such as *fib* Model Code 2010 (CEB-FIP 2013).

On the other hand, there have been considerable developments in weigh-in-motion (WIM) systems (Jacob and O'Brien 2005). It means that more accurate measurements of traffic volumes are now available, and it can be used to estimate the current traffic loading on the existing bridges.

Although many researchers have focused on the development of the prediction models of the current condition of the structural resistances and the traffic loads, both models are rarely combined. This study contributes to the development of a novel full-probabilistic safety assessment method for existing RC bridges. In the proposed method, chloride-induced corrosion of reinforcing steels is considered as the deterioration mechanism of RC bridges, and the resistances of the bridge components are evaluated as random variable. The traffic load models are derived from WIM data. As with the load models proposed in the major design codes, such as Eurocode 1, double-axle concentrated loads and uniformly distributed loads (UDLs) are separately modeled. Thereafter, the methodologies to apply the proposed method to finite element (FE) analysis, which is one of the most useful tools for calculating the structural behavior, are presented. Finally, as an illustrative case study, stochastic FE analysis is conducted, and the structural reliability of a RC deck slab of a box-girder bridge is calculated.

2. Deterioration Model

In the past decades, several models for chloride-induced steel corrosion have been developed and applied to certain standards, such as *fib* Model Code 2010 (CEB-FIP 2013). In this section, the methodologies to estimate corrosion amount of reinforcing steels are briefly summarized.

2.1 Corrosion initiation

According to *fib* Model Code 2010 (CEB-FIP 2013), the chloride concentration $C(x,t)$ at depth x from the concrete surface at time t can be appropriately calculated by Fick's second low as:

$$C(x,t) = C_s\left\{1 - erf\left(\frac{x}{2\sqrt{D_{app}\cdot t}}\right)\right\} \tag{1}$$

where C_s is the chloride concentration on the concrete surface, D_{app} is the apparent coefficient of chloride diffusion in concrete, and $erf(\cdot)$ is the error function. The apparent coefficient of chloride diffusion can be expressed as (Cao et al. 2013):

$$D_{app}(t) = k_e \cdot k_t \cdot D_c \cdot \left(\frac{t_0}{t}\right)^n \tag{2}$$

where k_e is the environmental factor, k_t is a parameter that considers the influence of test methods, which is assumed to be 1.0 in this study, D_c is the chloride migration coefficient, t_0 is the reference point of time (= 28 days), and n is the aging exponent.

It is assumed that reinforcing steels start corroded when the chloride concentration on the steel surface reaches the threshold value C_T. Therefore, the time to corrosion initiation t_{ini} is calculated from Eq. (1) and (2) as follows:

$$t_{ini} = \left[\frac{d^2}{4 \cdot k_e \cdot k_t \cdot D_c \cdot t_0^n} \left\{ erf^{-1}\left(1 - \frac{C_T}{C_S}\right) \right\}^{-2} \right]^{\frac{1}{1-n}} \quad (3)$$

The statistical parameters of each design variable are referred from CEB-FIP (2006) and Faber and Straub (2006).

2.2 Corrosion propagation

After corrosion initiation, corrosion products on the surface of reinforcing steels gradually increase at a certain rate. The corrosion rate is usually expressed by means of the corrosion current density i_{corr}, which can be estimated as a time-dependent variable as:

$$i_{corr}(t) = i_{corr}(1) \cdot \alpha (t - t_{ini})^{\beta} \quad (4)$$

where $i_{corr}(1)$ is the initial corrosion current density, and α and β are the constant coefficients. In general, corrosion rate may be effected by concrete quality and concrete cover depth. Therefore, in this study, the corrosion current density is expressed by means of *w/c* rate and concrete cover depth, *d*, as follows (Vu and Stewart 2000):

$$i_{corr}(1) = \frac{37.8(1 - w/c)^{-1.64}}{d} \quad (5)$$

If the corrosion rate is assumed to be constant with time, α and β should be equal to 1.0 and 0.0, respectively. On the other hand, if it is assumed that the corrosion rate can be changed with time, it becomes a time-dependent variable. In Vu and Stewart (2000), it is suggested that the formation of rust products on the steel surface will reduce the diffusion of the iron ions away from the steel surface, and as a result, the corrosion rate will also reduce with time. In this study, it is assumed that α equals to 0.85 and β equals to -0.29. The estimated corrosion current density can be directly related to the loss of reinforcing steels by Faraday's law, that is, 1 $\mu A/cm^2$ corresponds to 0.0116 mm/year.

3. Traffic Load Model

WIM data collected on two highway bridges as detailed in Table 1 are used to generate stochastic load models. Before analysing the data, the raw data are cleaned and filtered in order to remove some unreasonable data. Even though the original data are filtered, more than 98% remained in each data set. The gross vehicle weight (GVW) histograms of the filtered data are depicted in Fig. 1. Both of them show multi-modal properties, lower peak

Table 1. Summary of WIM data.

	WIM-B1	WIM-B2
Number of lanes	2	2
Number of directions	2	2
Total trucks	121,797	133,543
Max. GVW (t)	73.6	115.0
Max. number of axles	10	11

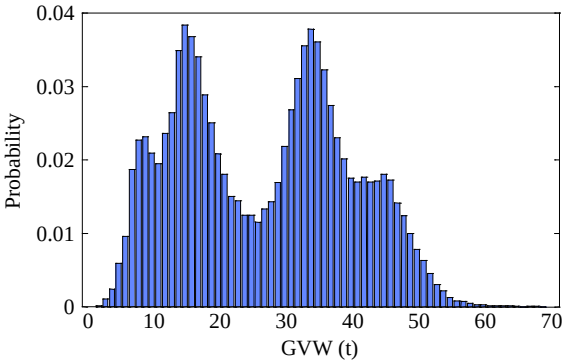

(a) WIM-B1

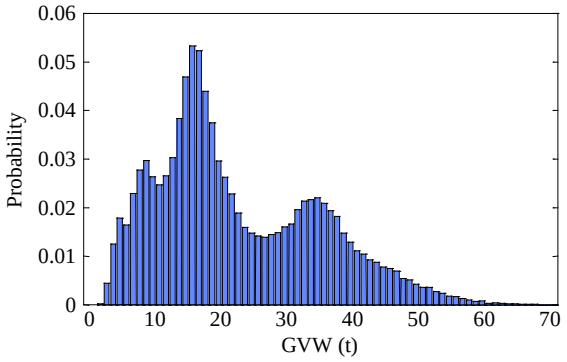

(b) WIM-B2

Figure 1. GVW histograms of filtered data.

of which (around 15 t) corresponds to empty trucks, while higher peak of which (around 35 t) corresponds to fully-loaded trucks. In addition, the data from WIM-B1 consist of more fully-loaded trucks comparing with those from WIM-B2.

For consistency with the major design codes, such as Eurocode 1, double-axle concentrated loads and UDLs are modeled using the WIM data. In the following sections, the methodologies to estimate each load are discussed. Since WIM data used in this study were obtained from 2-lane bidirectional (1 lane in each direction) highway bridges, traffic load models for more than a single lane in each direction cannot be established. Therefore, only one lane in each direction is considered hereafter.

3.1 Double-axle concentrated load

Double-axle concentrated loads are calculated for a 50m-long single-span bridge. Sagging moment at the mid-span is calculated as load effects. Maximum load effects resulting from the individual vehicles recorded in

WIM data are calculated using the influence line. The flow for calculating the maximum load effects by a vehicle is as follows:

1. place the first axle of a vehicle on an edge of the bridge;
2. calculate the load effects by each axle weight and store the sum of them as the maximum value;
3. move the vehicle forward (dx = 0.1 m) and calculate the total load effects;
4. if the current total load effect is greater than the maximum value, update the maximum load effect; and
5. repeat step 3 and 4 until the last axle of the vehicle reaches to the opposite edge of the bridge.

By repeating these steps for all vehicles, the maximum load effects resulting from the individual vehicles are obtained.

In fact, the load effects are affected by axle configurations such as the number of axles, axle spacing lengths, and axle weights. Considering an application to stochastic FE analysis, however, the configurations of axle loads should be fixed, otherwise, the mesh of the FE model has to be changed according to the axle configurations in every calculation run. Therefore, in this study, the configurations of concentrated loads are set in the same way as the Eurocode 1 (see Fig. 2).

The sagging moment at the midspan M_{mid} by double-axle with the axle spacing length of 1.2 m is calculated by:

$$M_{mid} = P \cdot \left(\frac{L}{4} + \frac{L/2 - 1.2}{2} \right) \tag{6}$$

where L is the span length and P is an axle load. Substituting the maximum load effects by the individual vehicles into Eq. (6), double-axle concentrated loads can be obtained. The histogram of the axle loads derived from WIM data is shown in Fig. 3. It can be seen that the axle loads have bi-modal distribution as with GVW.

In order to estimate stochastic models of the obtained axle loads, maximum likelihood estimation (MLE) method is used. In this case, bi-modal log-normal distribution, the probability density function of which is expressed as Eq. (7), is applied. The estimated stochastic model is also shown in Fig. 3 with the solid line, and the estimated parameters are shown in Table 3.

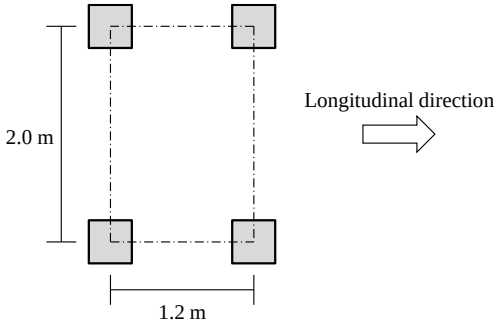

Figure 2. Configurations of double-axle loads.

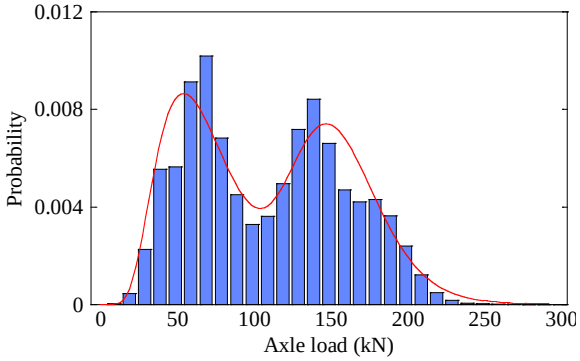

Figure 3. Histogram of axle load and estimated stochastic model (WIM-B1).

Table 2. Estimated model parameters for axle loads.

	w	λ_1	ζ_1	λ_2	ζ_2
	-	kN	kN	kN	kN
WIM-B1	0.56	4.16	0.199	5.00	0.032
WIM-B2	0.79	4.22	0.257	4.98	0.028

$$f(x) = w \cdot \frac{1}{\sqrt{2\pi}\zeta_1 x} \exp\left[-\frac{1}{2}\left(\frac{\ln x - \lambda_1}{2\zeta_1} \right)^2 \right] + (1-w) \cdot \frac{1}{\sqrt{2\pi}\zeta_2 x} \exp\left[-\frac{1}{2}\left(\frac{\ln x - \lambda_2}{2\zeta_2} \right)^2 \right] \tag{7}$$

3.2 Uniformly distributed load

For long span bridges, congested situation is the most critical, and the load distribution is close to be uniform (Nowak et al. 2010). In this study, UDL is calculated for only congested situation.

UDL is calculated from "virtual motorcades" derived from the statistical models of WIM data such as the proportion of vehicles, GVW and wheelbase (the sum of the axle spacing lengths). The flow for calculating UDL is as follows (also see Fig. 4):

1. divide all vehicles recorded in WIM data into several groups according to the number of axles, and calculate the composition rate of the groups;
2. estimate statistical models of GVW and wheelbase of each group;
3. select a vehicle by the composition rate, and assign the values of GVW and wheelbase with the estimated statistical models;
4. add vehicles with a certain clearance distance between the last axle of the previous vehicle and the first axle of the following vehicle until the total length of motorcade exceeds the span length of the bridge; and
5. divide the total weight of all vehicles in the motorcade by the span length to obtain the average UDL.

By repeating these steps, sufficient numbers of UDL samples are obtained, and the stochastic model of it can be estimated with MLE method.

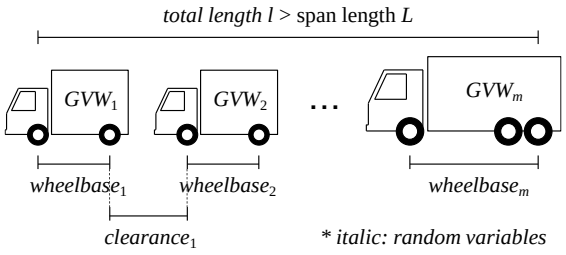

Figure 4. Image of "virtual motorcade".

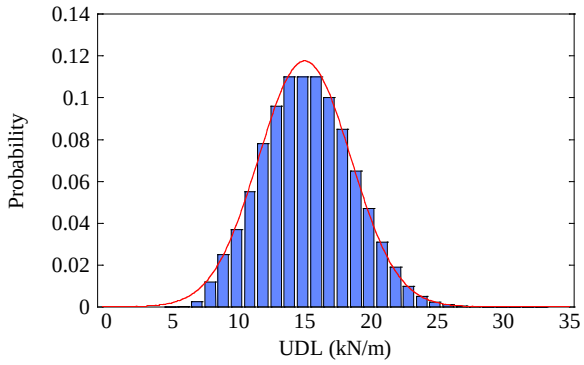

Figure 5. Histogram of UDL and estimated stochastic model (WIM-B1).

Table 3. Estimated model parameters for UDL.

	Mean	Standard deviation	COV
	kN/m	kN/m	-
WIM-B1	14.86	3.40	0.23
WIM-B2	12.72	3.34	0.26

As a result of MLE method, uni-modal normal distribution is applied to UDL. The histogram of UDL derived from WIM-B1 is shown in Fig. 5 with the estimated stochastic model (the solid line), and the estimated parameters are shown in Table 3.

4. FE Modelling for Corroded RC Structures

In order to apply the presented corrosion model to the assessment of RC bridges, three-dimensional FE model for corroded RC structures is proposed in this section. In this study, concrete and reinforcing steels are separately modeled in FE analysis. The concrete is modelled by three-dimensional solid element, while the reinforcing steels are modeled by two-node beam element. Moreover, the bond relation between concrete and reinforcing steels is represented by spring elements in the longitudinal direction of the reinforcing steels. The constitutive models for each material consider nonlinear behavior illustrated in Fig. 6.

As the corrosion mechanisms, the following effects by steel corrosion are considered in this study:

1. the cross-sectional reduction in reinforcing steels;
2. the reduction of the yield strength of reinforcing steels;
3. the reduction in concrete compressive strength; and
4. the reduction in the bond strength between concrete and reinforcing steels.

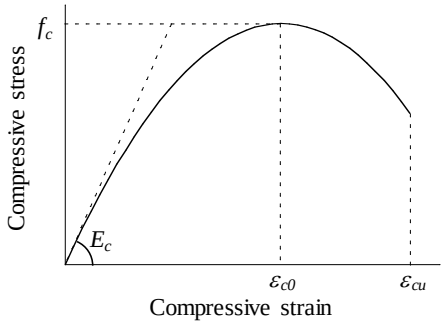

(a) Concrete under compression

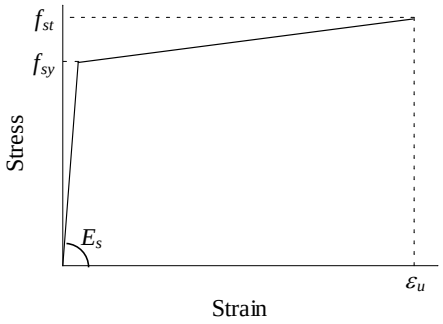

(b) Reinforcing steel

Figure 6. Constitutive relations.

4.1 Reinforcing steel

Uniform corrosion is considered and is modeled by reducing cross-sectional area and the yield strength of reinforcing steels. The remaining cross-sectional area of corroded reinforcing steels can be calculated by multiplying the corrosion rate η, which is estimated from the mass loss of the corroded steels, and the initial cross-sectional area of uncorroded steels A_0 as follows:

$$A_{res} = \eta A_0 = \frac{\pi \eta D_0}{4} \tag{8}$$

The reduced yield strength of reinforcing steels is generally expressed as follows:

$$f_{sy,res} = (1 - \alpha_{sy}\eta) f_{sy} \tag{9}$$

where $f_{sy,res}$ and f_{sy} are the reduced and the initial yield strength of reinforcing steels, respectively, and α_{sy} is the empirical coefficient. The coefficient has been obtained from several experimental results, and it is assumed to be 0.5 (Du et al. 2005)

4.2 Concrete

The concrete cover will be cracked by the expansion of corrosion products. The effect of cover cracking is taken into account by reducing the concrete compressive strength of the concrete cover. The reduced compressive strength is calculated as (Coronelli and Gambarova 2004):

$$f_{ck,res} = \frac{f_{ck}}{1 + K\,\varepsilon_1/\varepsilon_{c0}} \tag{10}$$

where $f_{ck,res}$ and f_{ck} are the reduced and the initial compressive strength of cover concrete, respectively, K is the coefficient related to the roughness and diameter of reinforcing steels (for medium-diameter ribbed bars, K = 0.1), ε_{c0} is the compressive strain at peak compressive stress, and ε_1 is the average tensile strain in the cracked concrete. The average tensile strain ε_1 is evaluated as (Coronelli and Gambarova 2004):

$$\varepsilon_1 = n_{bars} w_{cr} / b_0 \tag{11}$$

where n_{bars} is the number of compressive reinforcing steels in the section width b_0, and w_{cr} is the total crack width, which can be expressed as $w_{cr} = 2\pi x$ (Molina et al. 1993).

The corrosion pattern of concrete cover depends on the arrangement of reinforcing steels. Therefore, in this study, the residual model of concrete compressive strength is applied only to the concrete cover surrounding reinforcing steels as shown in Fig. 7.

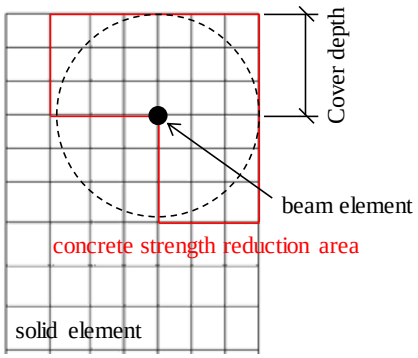

Figure 7. Concrete strength reduction area.

4.3 Bond relation

In this study, the local bond stress-slip relation model proposed in CEB-FIP (2013), as shown in Fig. 8, is adopted for uncorroded structures.

The bond stress-slip relation of corroded RC structures is complex and difficult to formulate. A wide range of experiments related to bond strength degradation have been conducted, and the following equation is proposed based on such experimental results in Bhargava et al. (2008):

$$\tau_b(s) = \beta \tau_{b0}(s) \tag{12}$$

where $\tau_b(s)$ is the bond stress between corroded reinforcing steels and concrete, $\tau_{b0}(s)$ is the bond stress between uncorroded reinforcing steels and concrete presented above, and β is the ratio of the bond strength at a certain corrosion rate to the initial (uncorroded) bond strength, as follows:

$$\beta = \begin{cases} 1.0 & \eta \le 1.5\% \\ 1.192e^{-11.7\eta} & \eta > 1.5\% \end{cases} \tag{13}$$

5. Illustrative Case Study

5.1 Model settings

As an illustrative case study, a box-girder bridge, which has a cross-section as shown in Fig. 9, is considered.

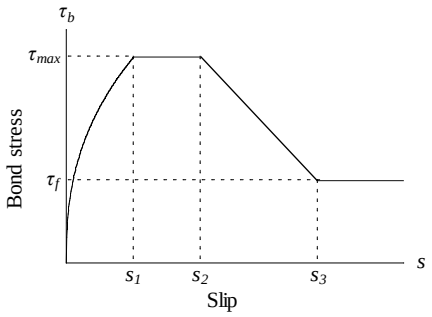

Figure 8. Local bond stress-slip relation.

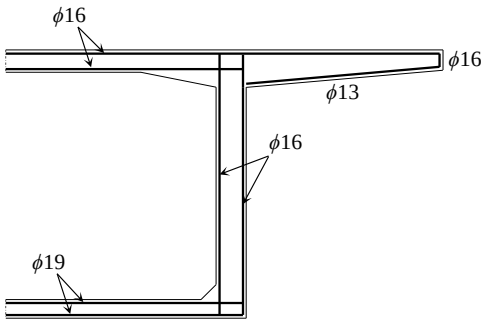

Figure 9 Cross-section of box-girder bridge.

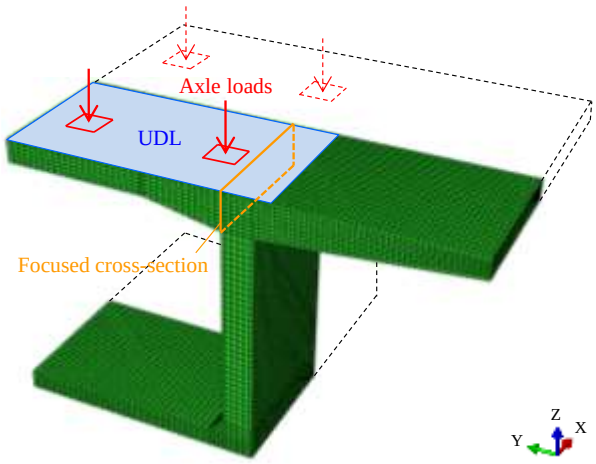

Figure 10. FE model.

Considering symmetry, only half of the cross-section is considered. It is reinforced, and the reinforcing steels are considered corroded due to chloride-ion ingress. The initial values of the compressive strength of concrete and the yield strength of reinforcing steels are assumed as 40 N/mm^2 and 345 N/mm^2, respectively.

The FE model is shown in Fig. 10. It has 44,561 nodes and 43,530 elements in total. Considering symmetry of the load configurations, only one axle load is applied to the FE model. The structural reliability of the deck slab is calculated at the joint of the deck and the web (see Fig. 10). The ultimate limit state for flexural strength is assumed to calculate the failure probability as:

$$g = \gamma M_u - M \tag{14}$$

where M_u is the ultimate capacity of the target structural section, M is the bending moment obtained from the FE analysis, and γ is a safety factor. To simplify, it is assumed that only the core (uncorroded) concrete and reinforcing steels are considered in the calculation of bending resistance, that is, the corroded concrete cover does not contribute to flexural strength. 1,000 simulation runs are conducted, and the probability of failure at the focused cross-section is calculated with Monte-Carlo method.

5.2 Reliability of RC deck slab

From the results of FE analysis, the stochastic distribution of the bending moment in the focused cross-section is obtained as shown in Fig. 11. It shows that the distributions obtained from WIM data show bi-modality, which is affected by axle load models.

For each load model, the probability of failure after 50 years of construction is calculated as shown in Table 4. Considering the structural safety, even the probabilities obtained from the proposed load models are relatively high and some maintenance actions have to be done in the early stage. However, the point is that the actual conditions of resistances and loads are reflected to the reliability analysis, and the structural safety can be quantitatively evaluated in terms of the probability of failure. In other words, using the proposed load models, the bridges under the different conditions can be quantitatively compared, and less conservative judgment for maintenance can be made.

6. Conclusions

This paper presented a full-probabilistic safety assessment method of existing bridges, and it was applied to FE analysis, which is one of the useful tools for calculating the structural behavior of RC structures. As the deterioration mechanism of RC structures, chloride-induced corrosion of reinforcing steels was considered, and the resistances of the bridge components were calculated as random variables. Meanwhile, WIM data were used to estimate stochastic traffic load models. As with the load models proposed in the major design codes, such as Eurocode 1, double-axle concentrated loads and uniformly distributed load were modeled using site-specific WIM data. Then, both models for predicting structural resistances and the traffic loads were applied to FE analysis to evaluate the structural reliability of the bridges.

As a result of this study, it was found that the structural reliability of existing bridges could be quantitatively evaluated in terms of the probability of failure. The proposed models can reflect the actual condition of existing bridges. Therefore, it allows to make more realistic decisions in maintenance process, leading to saving resources, such as time, budgets, and materials.

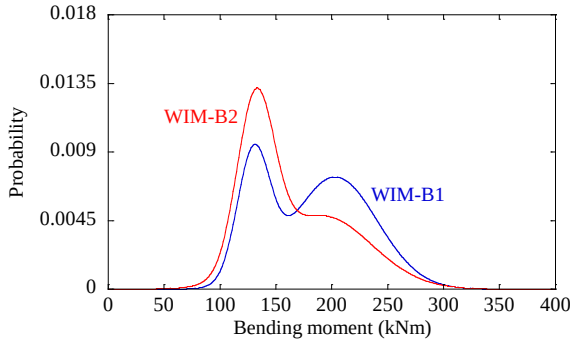

Figure 11. Bending moment.

Table 4. Probability of failure after 50 yrs.

	Mean	Standard deviation	COV
WIM-B1	0.012	0.0049	0.408
WIM-B2	0.014	0.0053	0.379

References

Bhargava, K., Ghosh, A.K., Mori, Y. and Ramanujam, S. 2008. Suggested empirical models for corrosion-induced bond degradation in reinforced concrete. *Journal of Structural Engineering*, 134(2): 221–230.

Cao, C., Cheung, M.M.S. and Chan, B.Y.B. 2013. Modelling of interaction between corrosion-induced concrete cover crack and steel corrosion rate. *Corrosion Science*, 69: 97–109.

CEB-FIP. 2006. *fib Bulletin 34: Model Code for Service Life Design*. International Federation for Structural Concrete, Lausanne.

CEB-FIP. 2013. *fib Model Code for Concrete Structures 2010*. International Federation for Structural Concrete, Lausanne.

Coronelli, D. and Gambarova, P. 2004. Structural assessment of corroded reinforced concrete beams: Modeling guidelines. *Journal of Structural Engineering*, 130(8): 1214–1224.

Du, Y.G., Clark, L.A., and Cham, A.H.C. 2005. Residual capacity of corroded reinforcing bars. *Magazine of Concrete Research*, 57(3): 135–147.

Faber, M.H. and Straub, D.A. 2006. Computational framework for risk assessment of RC structures using indicators. *Computer-Aided Civil and Infrastructure Engineering*, 21: 216–230.

Jacob, B. and O'Brien, E.J. 2005. Weigh-in-motion: Recent developments in Europe. In *Proceedings of the 4th International Conference on Weigh-In-Motion*, Taipei, Tai-wan, February 20–23, 2005.

Molina, F.J., Alonso, C. and Andrade, C. 1993. Cover cracking as a function of rebar corrosion: Part 2 – Numerical model. *Materials and Structures*, 26(9): 532–548.

Nowak, A.S., Lutomirska, M. and Sheikh Ibrahim, F.I. 2010. The development of live load for long span bridges. *Bridge Structures*, 6: 73–79.

Vu, K.A.T. and Stewart, M.G. 2000. Structural reliability of concrete bridges including improved chloride-induced corrosion models. *Structural Safety*, 22: 313–333.